The time domain in co-stained cell imaging: time-resolved emission imaging microscopy using a protonatable luminescent iridium complex

L. Murphy, A. Congreve, L.-O. Pålsson and J. A. G. Williams*

Department of Chemistry, University of Durham, Durham, DH1 3LE, U.K.

**E-mail: j.a.g.williams@durham.ac.uk*

1. Experimental and instrumental details

(i) NMR spectroscopy and mass spectrometry

^{1}H and ^{13}C NMR spectra were recorded on a Varian 700 MHz instrument. Chemical shifts (δ) are given in ppm and are referenced using the residual protio solvent resonance. Coupling constants (*J*) are in Hertz. Accurate mass spectra were obtained by electrospray ionisation using an LCT Premier XE spectrometer (Waters UK Ltd). Elemental analysis was performed using an Exeter Analytical E-440 elemental analyser.

(ii) Electrochemistry

Cyclic voltammetry was carried out in a background electrolyte of tetrabutylammonium tetrafluoro-borate (0.1 M) in acetonitrile. A μAutolab type III potentiostat was used, with computer control and data storage using GPES Manager software. A three-electrode assembly was used, consisting of a platinum wire counter electrode, platinum flag reference electrode, and a glassy carbon working electrode. The measurements were carried out in a glass cell charged with 2 mg of complex in 2 mL of electrolyte solution, pre-purged with dry nitrogen gas.

(iii) Optical spectroscopy in solution. Absorption spectra were measured on a Biotek Instruments XS spectrometer, using quartz cuvettes of 1 cm pathlength. Steady-state luminescence spectra were measured using a Jobin Yvon FluoroMax-2 spectrofluorimeter, fitted with a red-sensitive Hamamatsu R928 photomultiplier tube; the spectra shown are corrected for the wavelength dependence of the detector, and the quoted emission maxima refer to the values after correction. Samples for emission measurements were contained within quartz cuvettes of 1 cm pathlength modified with appropriate glassware to allow connection to a high-vacuum line. Degassing was achieved via a minimum of three freeze-pump-thaw cycles whilst connected to the vacuum manifold; final vapour pressure at 77 K was $< 5 \times 10^{-2}$ mbar, as monitored using a Pirani gauge.

Luminescence quantum yields were determined using $[Ru(bpy)_3]Cl_2$ in degassed aqueous solution as the standard, for which $\Phi_{lum} = 0.042$ [J. Van Houten and R. J. Watts, *J. Am. Chem. Soc.*, **1976**, *98*, 4853]; estimated uncertainty in Φ_{lum} is ± 20% or better.

The luminescence lifetimes of the complexes were measured by time-correlated single-photon counting (TCSPC), following excitation at 374.0 nm with an EPL-375 pulsed-diode laser. The emitted light was detected at 90˚ using a Peltier-cooled R928 PMT after passage through a monochromator. The estimated uncertainty in the quoted lifetimes is ± 10% or better.

(iv) Cell culture and steady-state fluorescence microscopy. Chinese hamster ovary (CHO) cells were maintained in exponential growth as monolayers in Ham's F-12 medium, supplemented with 10% foetal bovine serum and 1% penicillin and streptomycin. For microscopy, cells were seeded in 12-well plates containing glass coverslips, and allowed to grow to 60–80% confluence in an incubator set at 37°C and 5% CO_2. At this stage, the old medium was removed and replaced with fresh medium containing the appropriate dosage of complex, solubilised with 1% DMSO. Following incubation, the coverslips were removed and washed with sterile PBS, mounted on a microscope slide, and imaged immediately. Epifluorescence images were taken using a Zeiss Axiovert 200M epifluorescence microscope with a digital camera and were processed using the Zeiss Axiovision software. A ×40 oil-immersion objective lens was used. A G365 excitation filter was used throughout; the emission filter was a FITCem (515-565 nm) for the iridium complexes and a 660-710 (Comar) for Lysotracker Red (Invitrogen).

(v) Time-resolved microscopy was performed by excitation at 355 nm with the third harmonic of a Q-switched Nd:YAG laser (Elforlight UVFQ-100-1-Y-355) producing optical pulses with a temporal width ~4 ns (FWHM) at 2 kHz. The microscope was a Leica 135 Axiovert epifluorescence instrument, in which the laser light was fed in through a beam expander and focused onto the sample using long working-distance objective lenses (Zeiss LD plan neofluar). The photoluminescence signal was detected, after passage through a dichroic mirror and long-pass filter, using a time-gated CCD camera (Imagex nano CCD) with a resolution of 752 × 582 pixels. In the excitation–detection sequence, the CCD camera control unit was used to trigger the Q-switch of the laser system with a TTL pulse. The luminescence decays were recorded using a constant acquisition time gate with 16 different delay times between excitation and detection.

(vi) Flow cytometric analysis was conducted using a DakoCytomation Inc. MoFlo multi-laser flow cytometer operating at 60 psi with a 70 μm nozzle. Samples were interrogated with a 100 mW 488 nm solid-state laser (propidium iodide, PI) or a 50 mW 355 nm laser (iridium complexes). The luminescence was detected through a 530/40 nm (iridium complexes) or a 470/30 nm (PI) bandpass filter, and the signal collected in logarithmic mode. The data were analysed using FlowJo software version 7.5 (Tree Star Inc.). Cells for flow cytometry were detached from the 12-well plates by incubation with trypsin (200 μL) for 3 min at 37°C. The cell suspension was placed in a centrifuge tube. The well was washed with medium (1 mL); the washing was added to the centrifuge tube and spun at 1500 rpm for 3 min. The supernatant was removed from the cell pellet, which was re-suspended in sterile PBS (2 mL) and placed on ice until flow cytometric analysis. For the PI-stained dead cell analysis, the PI was added to the cell suspension 5 min prior to analysis. Immediately prior to the analyses, the cell suspension was filtered through a 40 μm filter to remove any cell clumps.

2. Synthetic procedures and characterisation

$[Ir(ppy)_2(pybz)]$ – complex 1

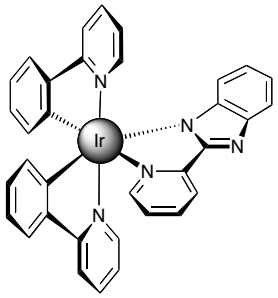

The procedure adopted was similar to that described by Zhu and co-workers for a somewhat related isoquinolyl complex [Y.-H. Sun, X.-H. Zhu, Z. Chen, Y. Zhang and Y. Cao, *J. Org. Chem.,* 2006, **71**, 6281]. A mixture of 2-pyridylbenzimidazole (40 mg, 0.21 mmol), $[Ir(ppy)_2(\mu\text{-}Cl)]_2$ (120 mg, 0.11 mmol), and potassium carbonate (85 mg, 0.62 mmol) in DMF (3 mL) was degassed prior to being refluxed under an atmosphere of nitrogen for 24 h. After allowing to cool to ambient temperature, water (10 mL) was added, and the resulting precipitate was separated by centrifugation, and washed with water (3 x 5 mL). The yellow solid was dissolved in CH_2Cl_2, the solution dried over $MgSO_4$, filtered, and the solvent removed under reduced pressure. Recrystallisation from THF led to the title compound (118 mg, 77%). Despite the use of a high-field spectrometer, reliable assignment of the ^1H NMR resonances to specific protons has not proved possible for complex **1**, owing to the significant but small difference between the two ppy ligands and the extensive overlap of cross peaks in the 2D spectra. ^1H NMR (700 MHz, $CDCl_3$): δ_H = 8.65 (1H, d, *J* = 6.5), 7.84 – 7.77 (4H, m), 7.75 (1H, d, *J* = 8.5), 7.69 (1H, d, *J* = 5.5), 7.67 – 7.65 (2H, m), 7.62 – 7.58 (2H, m), 7.55 (1H, td, J = 7.5, 1.0), 7.11 – 7.05 (2H, m), 7.03 (1H, td, J = 7.5, 1.0), 6.99 (1H, td, *J* = 7.5, 1.0), 6.92 – 6.87 (2H, m), 6.82 – 6.75 (3H, m), 6.45 (2H, m), 6.15

(1H, d, J = 8.5). ^{13}C NMR (176 MHz, $CDCl_3$): δ_C = 168.8, 168.6, 162.7, 155.3, 150.2, 149.7, 149.6, 148.7, 144.7, 144.3, 144.1, 138.0, 137.1, 136.7, 132.6, 132.4, 130.5, 129.8, 124.6, 124.3, 123.1, 122.8, 122.3, 122.0, 121.8, 121.6, 121.4, 119.0, 118.8, 118.7, 116.0. HRMS (ES+): *m/z* = 696.1714 ($M+H^+$). Calcd for $C_{35}H_{25}N_5{}^{191}Ir$ *m/z* = 694.1716. Found: C, 60.1; H, 4.0; N, 9.8 %. Calcd for $C_{35}H_{24}N_5Ir$: C, 60.5; H, 3.6; N, 10.1 %.

[Ir(ppy)$_2$(pybzH)](PF$_6$) – complex 2

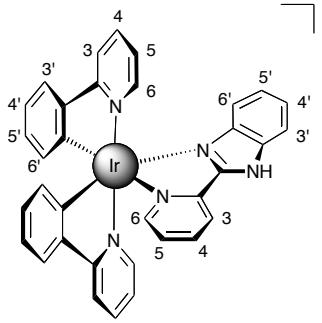

A solution of 2-pyridylbenzimidazole (45 mg, 0.23 mmol) in dichloromethane (5 mL) was added to a suspension of [Ir(ppy)$_2$(μ-Cl)]$_2$ (100 mg, 0.09 mmol) in methanol (4 mL). The resulting mixture was heated under reflux with stirring for 24 h, after which, the solvent was removed under reduced pressure. The residue was dissolved in a mixture of acetonitrile and water (1 mL of each), centrifuged to remove a small amount of insoluble material, and the clear solution then added dropwise to a saturated aqueous solution of KPF_6. The bright yellow precipitate which formed was collected by centrifugation, washed with water (3 × 5 mL), and dried under vacuum. The product was recrystallised from an acetonitrile / ether mixture (106 mg, 70%). In the NMR assignment, A and B respresent the two different ppy ligands, though it has not been possible to identify unequivocally which is which. ^{1}H NMR (700 MHz, $CDCl_3$): δ_H = 12.20 (1H, s, NH), 8.69 (1H, d, J = 7.5, $H^{3\ pybzH}$), 8.05 (1H, t, J = 7.5, $H^{4\ pybzH}$), 7.90 – 7.88 (2H, m, $H^{6\ pybzH}$ and $H^{3\ ppyA/B}$), 7.85 (1H, d, J = 8.0, $H^{3\ ppyA/B}$), 7.81 (1H, d, J = 8.0, $H^{3'\ pybzH}$), 7.72 (1H, m, $H^{4\ ppyA/B}$), 7.69 – 7.67 (3H, m, $H^{4\ ppyA/B}$, $H^{3'\ ppyA+B}$), 7.64 (1H, d, J = 5.5, $H^{5\ ppyA/B}$), 7.46 (1H, d, J = 5.5, $H^{5\ ppyA/B}$), 7.36 (1H, t, J = 7.5, $H^{5\ pybzH}$), 7.32 (1H, t, J = 8.0, $H^{4'\ pybzH}$), 7.08 (1H, t, J = 7.5, $H^{4'\ ppyA/B}$), 7.04 (1H, t, J = 7.5, $H^{4'\ ppyA/B}$), 6.98 (1H, t, J = 8.0, $H^{5'\ pybzH}$), 6.96 – 6.91 (4H, m, $H^{5'\ ppyA+B}$ and $H^{6\ ppyA+B}$), 6.41 (1H, d, J = 7.5, $H^{6'\ ppyA/B}$), 6.36 (1H, d, J = 7.5, $H^{6'\ ppyA/B}$), 6.21 (1H, d, J = 8.0, $H^{6'\ pybzH}$). ^{13}C NMR (176 MHz, $CDCl_3$): δ_C = 168.6, 168.3, 152.5, 151.2, 151.1, 149.9, 148.7, 148.1, 146.9, 144.4, 144.3, 140.5, 140.0, 138.2, 138.1, 134.8, 132.8, 132.1, 131.2, 130.5, 128.1, 126.8, 125.6, 125.2, 124.9, 124.8, 123.6, 123.4, 123.0, 122.9, 119.8, 119.7, 117.7, 114.9. HRMS (ES+): *m/z* = 696.1711 (M^+). Calcd for $C_{35}H_{25}N_5{}^{191}Ir$ *m/z* = 694.1716.

Note: Both complexes comprise a racemic mixture of Δ and Λ enantiomers, which were not separated. It is, of course, quite likely that they may interact differently with biomolecules in the cell.

3. Absorption and emission spectra

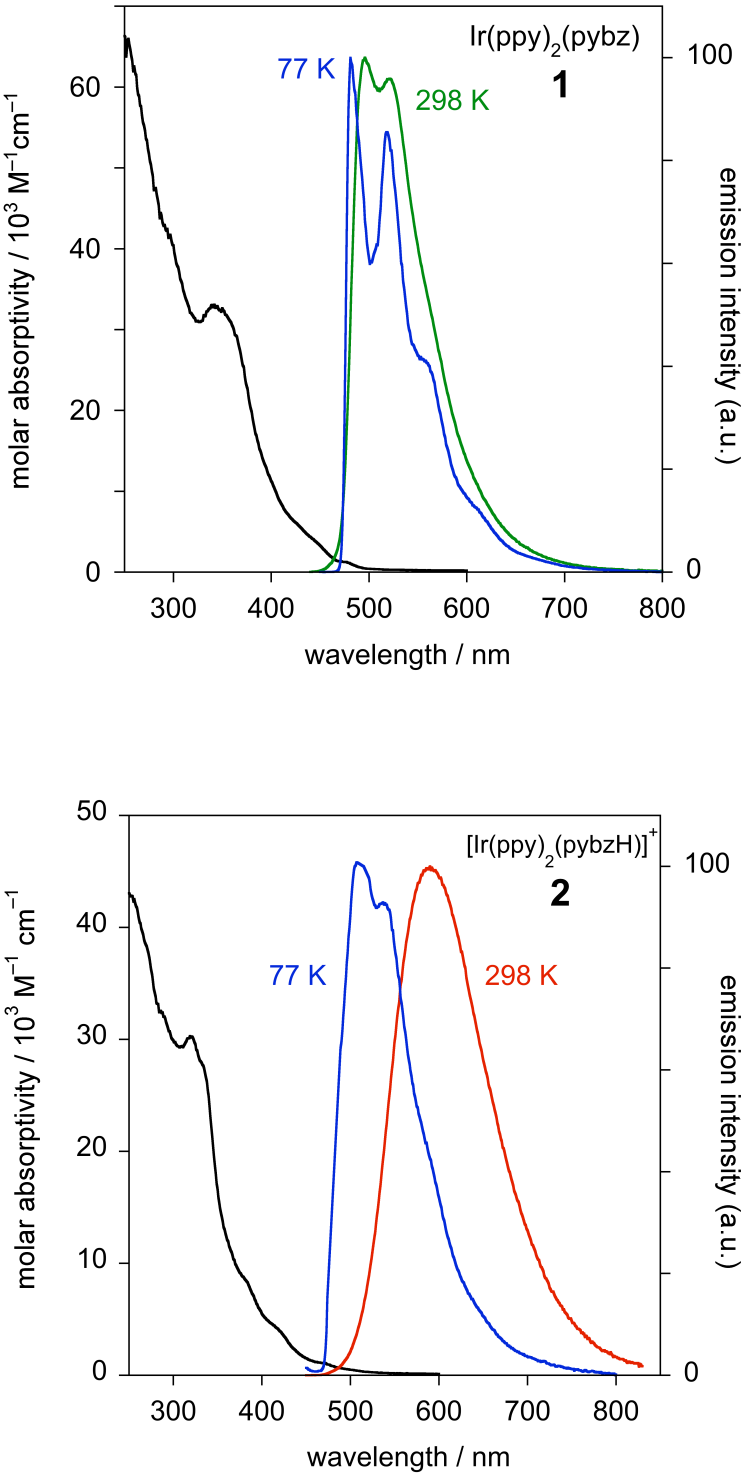

Fig. S1 Absorption and emission spectra of complexes **1** and **2** at 298 K in CH_2Cl_2 and emission spectra at 77 K in diethyl ether / isopentane / ethanol (2:2:1, v/v).

4. Cyclic voltammetry

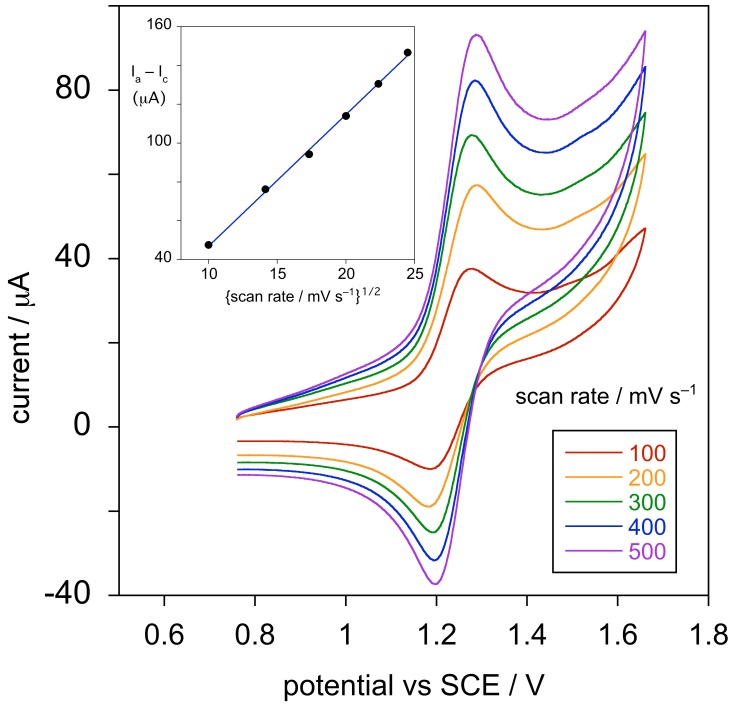

Fig. S2 Cyclic voltammogram of complex **1** in MeCN at 298 K, using Bu_4NPF_6 as the supporting electrolyte, showing the reversible oxidation wave. The inset shows the current varying linearly with the square root of the scan rate. The reduction was outside the available potential window.

5. pH titration

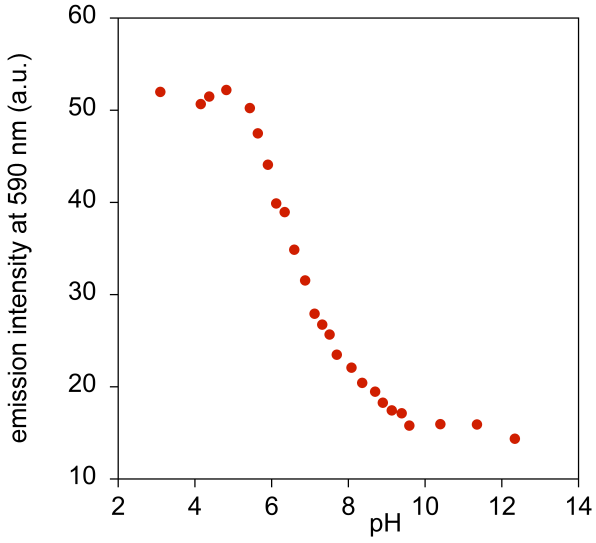

Fig. S3 Variation of the emission intensity of complex **1** in DMSO / H_2O (1:1) as a function of pH. Trifluoroacetic acid and sodium hydroxide were used as acid and base respectively. The same profile was observed starting from the pre-formed sample of **2**.

6. Fluorescence microscopy images for cells dosed with complexes 1, 2 and Lysotracker Red

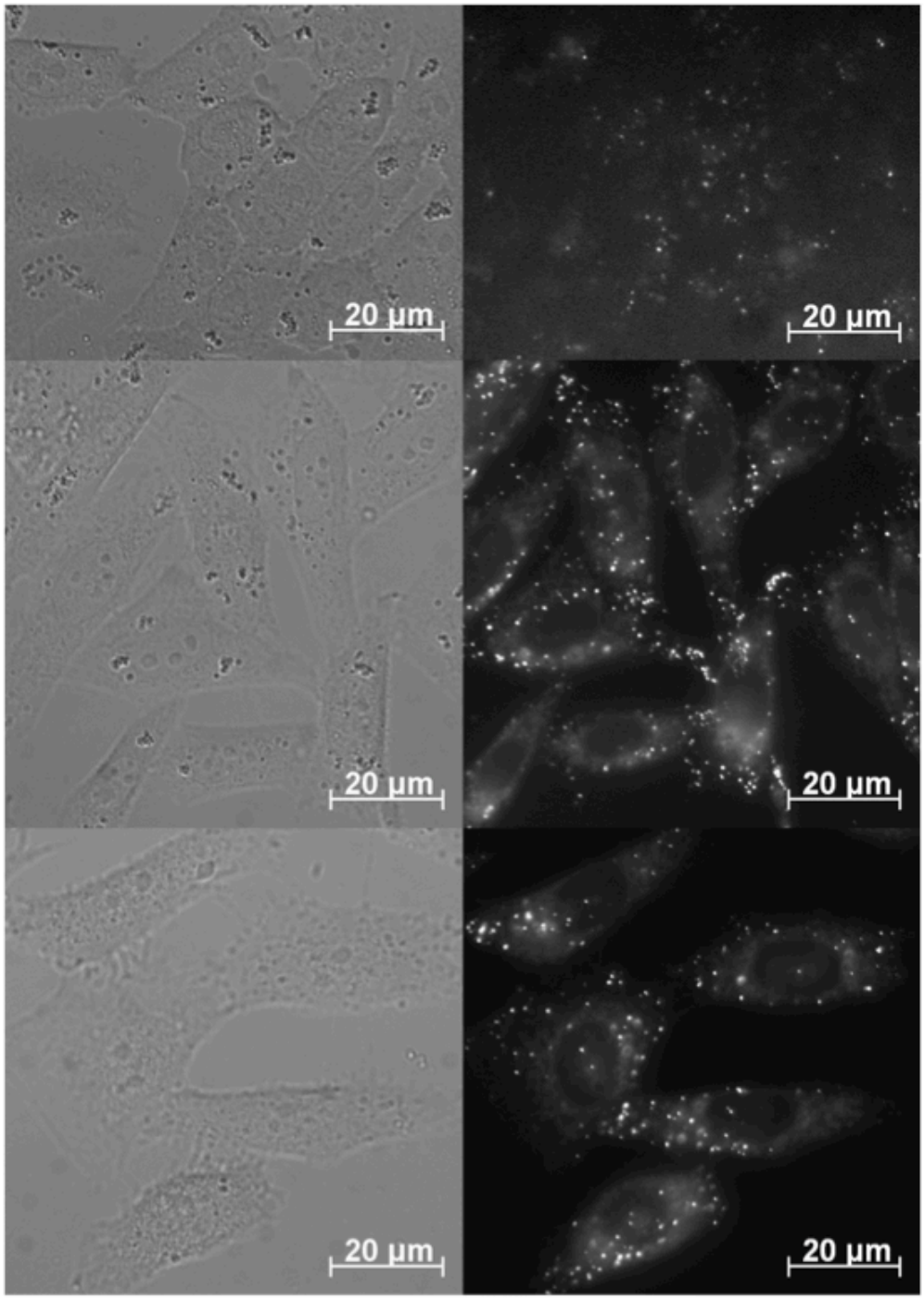

Fig. S4 Bright field (left) and fluorescence microscopy images (right) of CHO cells dosed with: *(a)* Lysotracker Red (80 nM, 30 min); *(b)* complex **1** (10 µM, 5 min); *(c)* complex **2** (10 µM, 1 h). Excitation and emission filters were G365 and FITCem respectively, except for (a) where a 660–710 nm emission filter was employed.

7. Fluorescence microscopy images for 1 in CHO cells after different incubation times

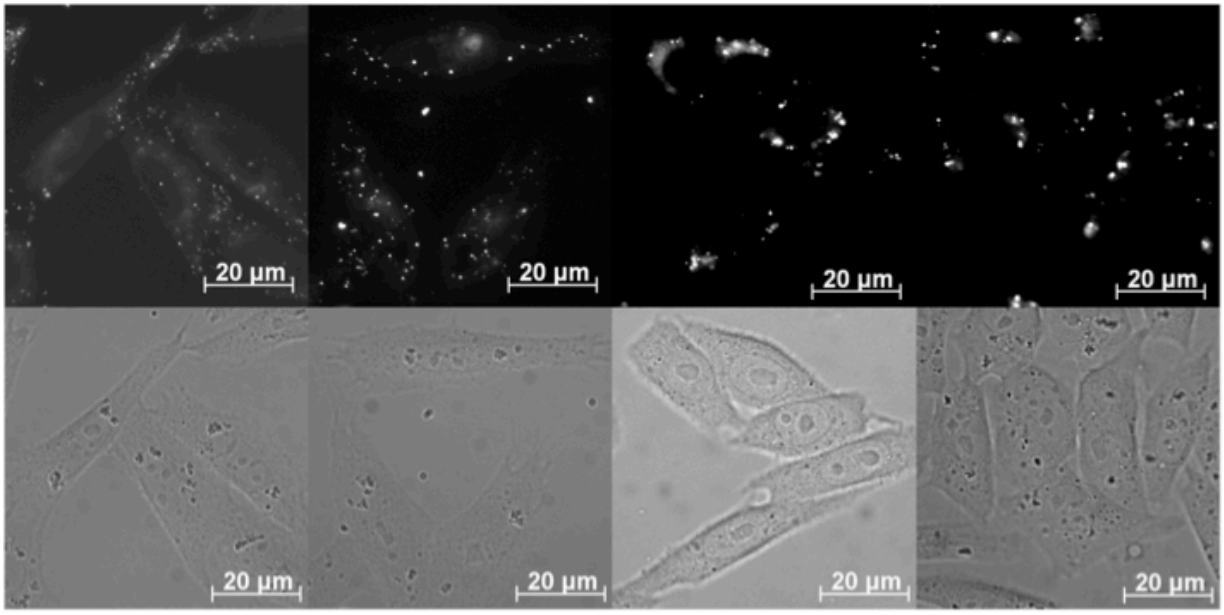

(a) **(b)** **(c)** **(d)**

Fig. S5 Comparative fluorescence (top) and bright field (bottom) images of CHO cells dosed with complex **1** (10 µM) for varying incubation times: (a) 5 min; (b) 1 h; (c) 4 h; (d) 24 h. The fluorescence microscopy images were acquired using a G365/FITCem filter set.

8. Effect of incubation temperature

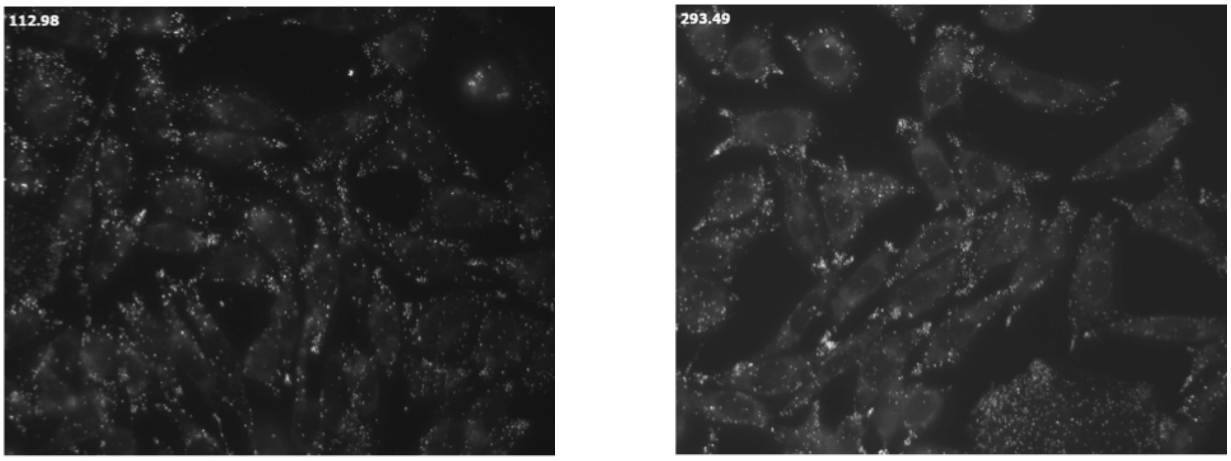

Fig. S6 Images of CHO cells dosed with 10 µM solutions of complex **1** (left) or complex **2** (right) at 4°C for 1 h, revealing the distibution to be similar to that observed following incubation at 37°C.

9. Flow cytometry data

(a) Complex 1

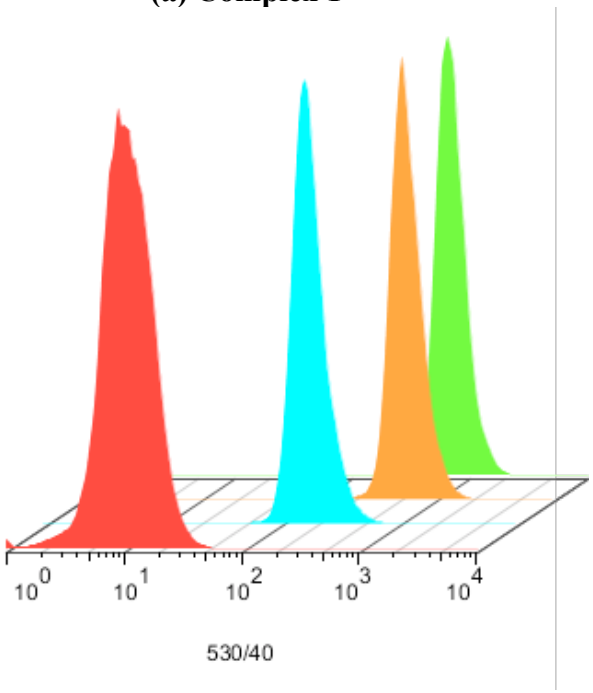

(b) Ir(ppy)$_3$

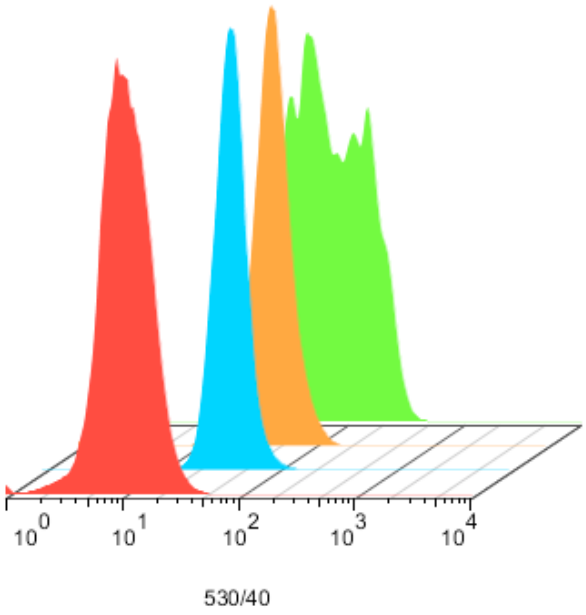

Fig. S7 Histograms showing the number of cells vs. the luminescence intensity (λ_{em} = 530–40 nm), *shown on a logarithmic scale,* for CHO cells incubated for 1 h with varying concentrations of complex **1** (a, top); and Ir(ppy)$_3$ (b, bottom). The colours correspond to the following dosage concentrations: red = unlabelled cells (control); blue = 10 μM; orange = 100 μM; green = 1 mM.

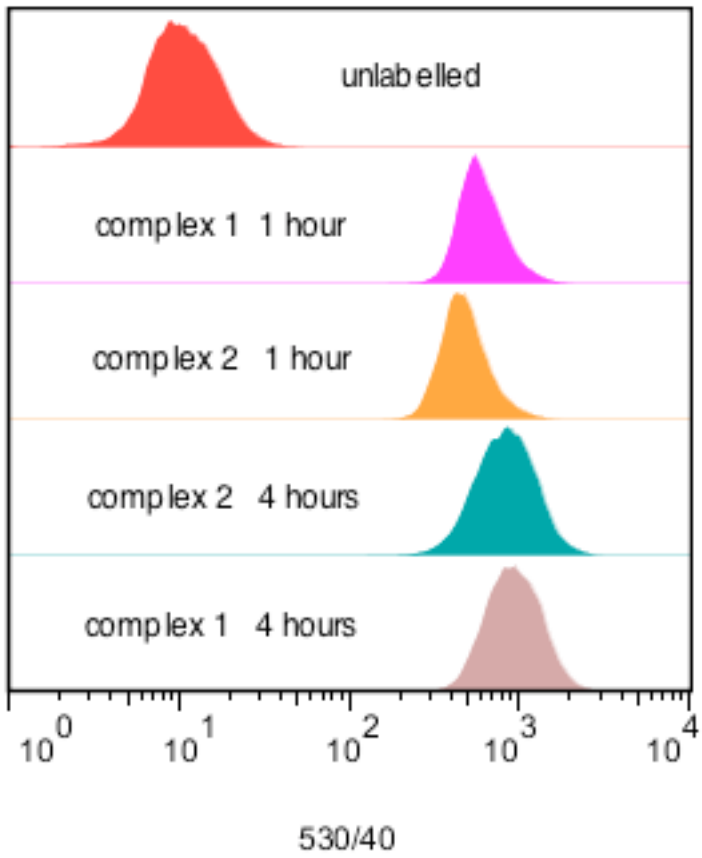

Fig. S8 Histograms showing the number of cells vs. the luminescence intensity (λ_{em} = 530/40 nm) for CHO cells incubated with **1** or its protonated form **2** (100 μM in each case) for 1 or 4 hours, highlighting that essentially identical results are obtained with either form (see text).

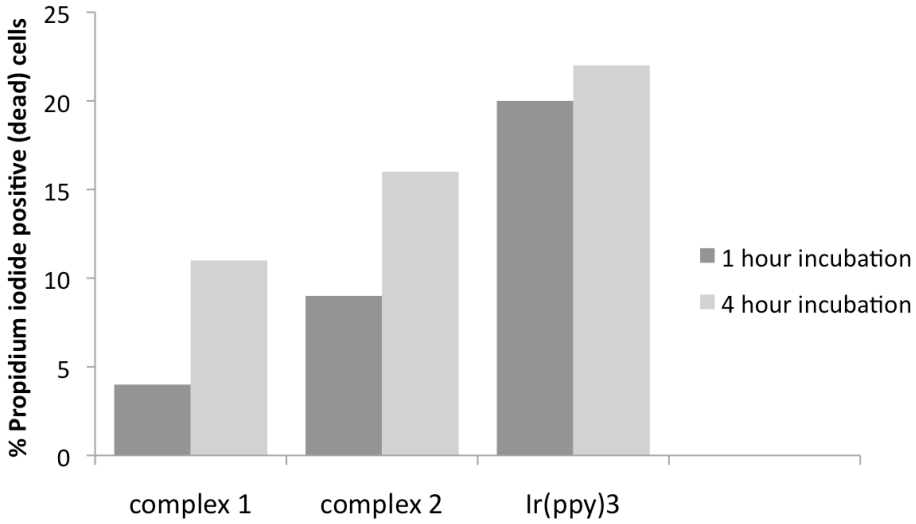

Fig. S9 Flow cytometric assessment of % dead cells using propidium iodide, upon incubation of CHO cells with **1**, or **2**, or $Ir(ppy)_3$ for 1 h or 4 h (100 μM in each case). [The higher toxicity upon incubation with **2** compared to **1** may be associated with the presence of the PF_6^- anion in **2**].

10. Spectra from cells dosed with complex 1 or complex 2

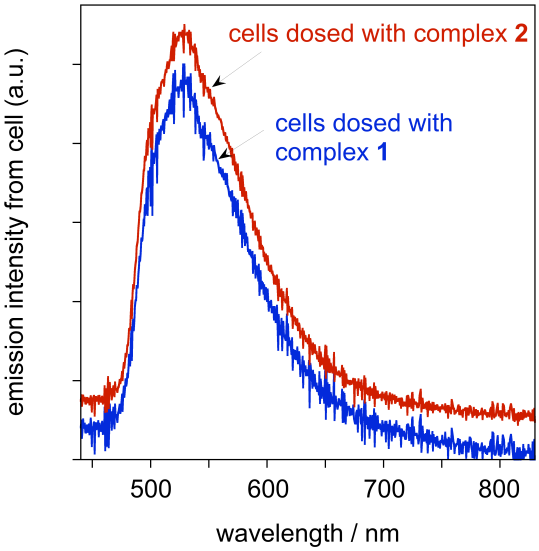

Fig. S10 Emission spectra obtained from CHO cells dosed with either complex **1** or with complex **2** under identical conditions (incubation with 10 μM solution for 5 min at 37°C), revealing that identical spectra – similar to that of **1** in solution – are obtained in each case.

11. Emission spectra of 1 and 2 in solvents of varying polarity at 298 K

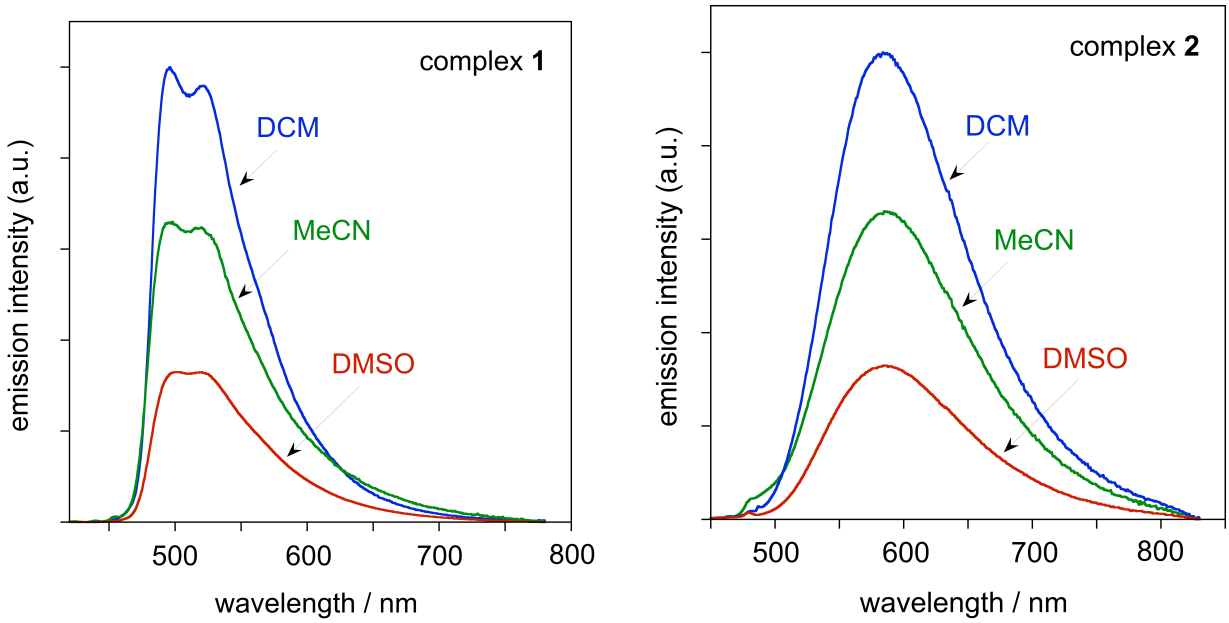

Fig. S11 Emission spectra of **1** (left) and **2** (right) in DCM, MeCN, and DMSO (dielectric constants = 8.9, 37.5, 46.7 respectively), revealing the absence of significant solvatochromism. These observations rule out the possibility that the spectrum observed for **2**-dosed cells could arise from the cationic form blue-shifted by the local environment. [Trifluoroacetic acid (10 μL) has been added to the sample of **2** in DMSO, as the complex is substantially deprotonated in the pure solvent].

12. Time-resolved emission within CHO cells

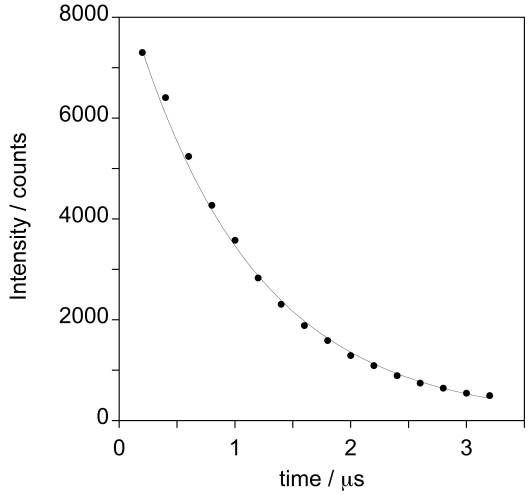

Fig. S12 Typical emission kinetic trace obtained by monitoring the emission from a perinuclear region of CHO cells dosed with complex **1** (in this instance, incubation with a 10 μM solution for 1 h). The solid line represents the monoexponential fit to the experimental data points, which were acquired using a time gate of 200 ns for each time delay after the excitation pulse.

The kinetic decay of emission from cells loaded with *fac*-Ir(ppy)$_3$ was also recorded. Despite the emission being weaker, there was sufficient intensity to determine the lifetime to be 0.9 ± 0.2 μs.